Viscoplastic Displacement Flow in a Vertical Pipe

Nasim Kazemi, Soheil Akbari, David Vidal, Seyed Mohammad Taghavi

Dept. of Mechanical Engineering –Polytechnique Montréal, Montréal, QC, Canada

Dept. of Chemical Engineering – Université Laval, Québec, QC, Canada

Introduction

Industrial motivations:

- There has been an increase of 56% in energy consumption from 2010 to 2040.
- The world is still highly dependent on fossil fuels.
- Canada requires enhancing oil & gas industries as one of the global energy providers.

Applications of displacement flows in the oil and gas industry:

- Primary well cementing
- Plug and abandonment

Advantages of primary well cementing:

- Creating hydraulic seal and zonal isolation
- Preventing fluids' contamination
- Supporting well and casing mechanically
- Protecting water-producing zones
- Preventing corrosion of the casing

Different stages of primary well cementing:

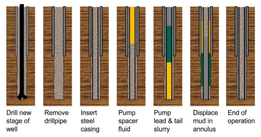

Figure 1 Schematic of the stages of mud removal in primary well cementing [1].

Properties of cement slurry:

Generally, cement slurry behaves as a non-Newtonian fluid. For oilfield purposes, it is mainly considered a viscoplastic fluid. Cement slurry shows a variety of complex flow behaviors. Thus, there are several models to predict cement behavior. However, for oilfield purposes, mainly Herschel-Bulkley model is considered [6]. It is described as below.

Herschel-Bulkley model:

$$\begin{cases} \hat{\tau} = \hat{\tau}_y + \hat{\kappa}\hat{\dot{\gamma}}^n & \hat{\tau} > \hat{\tau}_y \\ \hat{\dot{\gamma}} = 0 & \hat{\tau} \le \hat{\tau}_y \end{cases}$$

Literature Review

Authors	Flow type	Fluids types	Geometry	Inclination	Geometry Movement	*At*	*m*	Approach
Lyu *et al.* 2018 [2]	Exchange	Newtonian	Pipe, $\hat{H} = 3\ m$, $\hat{R} = 9.5\ mm$	65 – 85 degrees from vertical	0-7.33 rad/s	0.0035 – 0.01	1	Experimental & numerical
Amiri *et al.* 2018 [3]	Imposed	Newtonian	Pipe, $\hat{H} = 3\ m$, $\hat{R} = 9.5\ mm$	Vertical	oscillation	(0.001-7) $\times 10^{-2}$	1	Experimental
Lyu & Taghavi 2020 [4]	Imposed	Newtonian	Pipe, $\hat{H} = 3\ m$, $\hat{R} = 9.5\ mm$	60 – 83 degrees from vertical	0-7.33 rad/s	(1.5, 5.5, 10) $\times 10^{3}$	1	Experimental
Lyu & Taghavi 2020 [5]	Imposed	Yield stress displaced fluid	Pipe, $\hat{H} = 3\ m$, $\hat{R} = 9.5\ mm$	60 – 80 degrees from vertical	0-6.28 rad/s	0.0035-0.02	Large	Experimental

Experimental approach

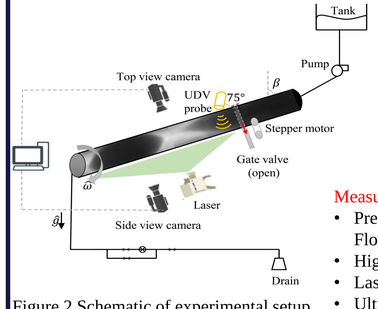

Figure 2 Schematic of experimental setup.

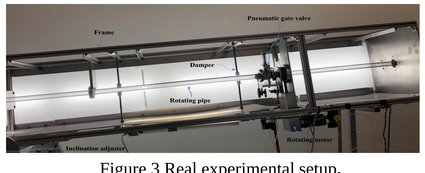

Figure 3 Real experimental setup.

Measurement tools:

- Precious scale, Density meter, pH-meter, Rheometer, Flow meter.
- High speed camera
- Laser induced Fluorescence (LIF)
- Ultra doppler velocimetry (UDV)

Numerical approach

Geometry & Boundary conditions:

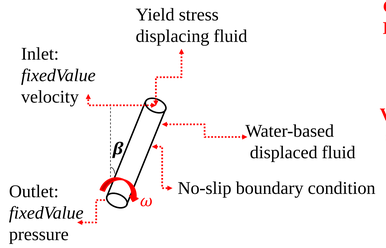

Governing Equations:

$$\frac{\partial c}{\partial \hat{t}} + \nabla \cdot (c\hat{u}) = 0$$

$$\nabla \cdot \hat{u} = 0$$

$$\frac{\partial \hat{\rho}\hat{u}}{\partial \hat{t}} + \nabla \cdot (\hat{\rho}\hat{u}\hat{u}) = -\nabla \hat{p} + \nabla . \hat{\tau} + \hat{\rho}\hat{g}$$

Viscoplastic displacing Fluid: Herschel-Bulkley model; Regularized model

Solution: OpenFOAM; InterFoam solver; VOF methods for interface tracking; Compute Canada

Ranges of variables and regime classification

Parameter	Name	Definition	Range or value
n	Power-Law index	-	$0.4 - 0.7$
At	Atwood number	$\frac{\hat{\rho}_H - \hat{\rho}_L}{\hat{\rho}_H + \hat{\rho}_L}$	$10^{-3} - 7 \times 10^{-2}$
B	Bingham number	$\frac{\hat{\tau}_y \hat{R}}{\hat{\mu}_H \hat{V}_0}$	$0.17 - 0.83$
M	Viscosity ratio	$\frac{\hat{\mu}_L}{\hat{\mu}_H}$	$2 \times 10^{-5} - 0.0105$
Pe	Peclet number	$\frac{\hat{V}_0 \hat{R}}{\hat{D}_m}$	$4 \times 10^{3} - 59 \times 10^{5}$
Re	Reynolds number	$\frac{(\hat{\rho}_H + \hat{\rho}_L)\hat{V}_0 \hat{R}}{2\hat{\mu}_H}$	$5 \times 10^{-4} - 10.73$
Fr	Froude number	$\frac{\hat{V}_0}{\sqrt{At\hat{g}\hat{R}}}$	$0.097 - 14.55$

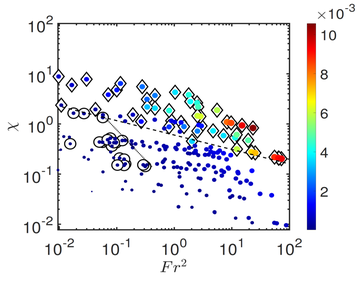

Figure 5 Regime classification in the plane of χ versus Fr^2. The color bar and the size of the data points represents the viscosity ratio. The separation and the mixing regime data points are surrounded by circle and diamond, respectively. Data points without any surrounded symbols are related to the plug flow regime. The dashed and dotted lines represent the transition from mixing regime to separation or plug flow regimes and from separation to plug flow, respectively.

Efficient displacement flow regime: The Balance between characteristic inertial stresses and the characteristic buoyant stresses:

$$\frac{1}{2}(\hat{\rho}_H + \hat{\rho}_L)\hat{V}_0{}^2 \sim (\hat{\rho}_H - \hat{\rho}_L)\hat{g}\hat{R} \Rightarrow \frac{(\hat{\rho}_H + \hat{\rho}_L)\hat{V}_0{}^2}{2(\hat{\rho}_H - \hat{\rho}_L)\hat{g}\hat{R}} = Fr^2$$

The removal of the displaced fluid in the longitudinal direction: The Balance between viscous stresses and the buoyant stresses:

$$\frac{\hat{\mu}_H \hat{V}_0}{\hat{R}} \sim (\hat{\rho}_H - \hat{\rho}_L)\hat{g}\hat{R} \Rightarrow \frac{(\hat{\rho}_H - \hat{\rho}_L)\hat{g}\hat{R}^2}{\hat{\mu}_H \hat{V}_0} \approx \chi$$

Results

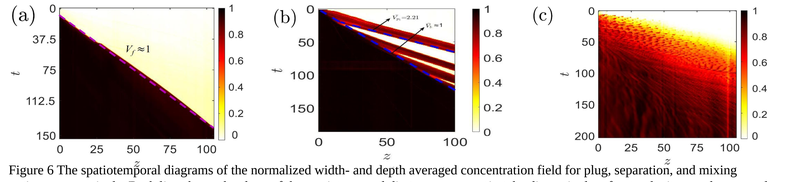

Figure 6 The spatiotemporal diagrams of the normalized width- and depth averaged concentration field for plug, separation, and mixing regimes, respectively. Dash line shows the slope of the spatiotemporal diagram, representing the dimensionless front velocity. t and z are made dimensionless using pipe radius and imposed velocity.

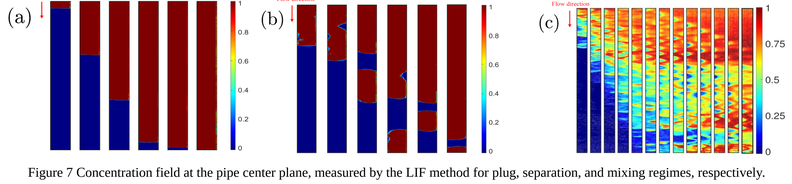

Figure 7 Concentration field at the pipe center plane, measured by the LIF method for plug, separation, and mixing regimes, respectively.

Results

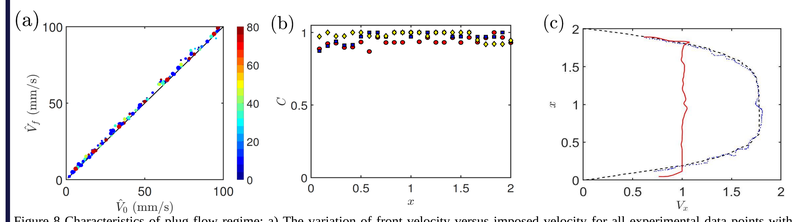

Figure 8 Characteristics of plug flow regime: a) The variation of front velocity versus imposed velocity for all experimental data points with the plug flow behavior. Color bar indicates the value of density difference (kg/m^3) and the size of the symbols shows the yield stress. b) The average concentration of heavy fluid over the diameter of the pipe when the front reaches the end of the flow domain at a specific time at 3 different pipe lengths. c) The axial velocity component for the time when the front is passing the location of UDV probe. The experimental axial velocity components are distorted because of the avoid less noises and perturbations near the walls so they are removed. The dashed black and blue line represents the analytical and experimental velocity profile for single phase Herschel-Bulkley fluid inside the pipe.

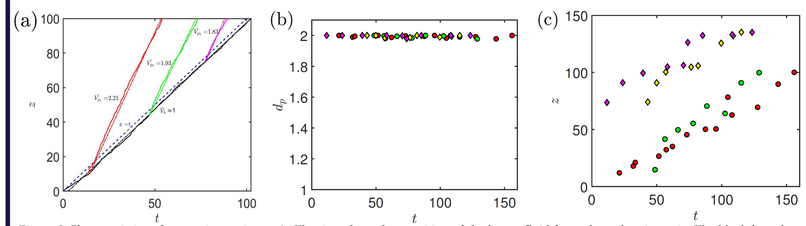

Figure 9 Characteristics of separation regime : a) The time dependent position of the heavy fluid front along the pipe axis. The black line shows the velocity of bulk fluid. The colored lines represent the separated pieces. The dashed lines are the linear fits to the datapoints. b) The dimensionless diameter of the separated pieces versus the dimensionless time of the experiments. c) The dimensionless distance of separation point from the gate valve versus the dimensionless time of the experiments. Datapoints at b) and c) have the same imposed velocity of $\hat{V}_0$~7 mm/s and the density differences of circle and diamond datapoints are 19.5 and 5.11 *kg/m*^{3}, respectively.

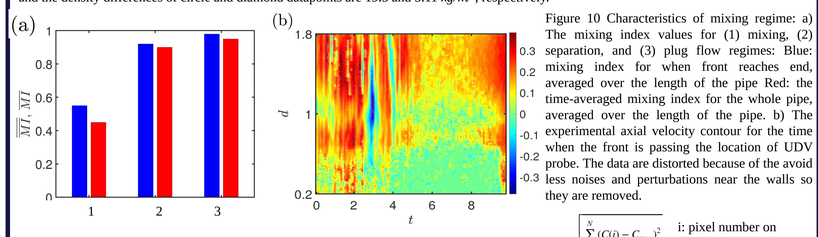

Figure 10 Characteristics of mixing regime: a) The mixing index values for (1) mixing, (2) separation, and (3) plug flow regimes: Blue: mixing index for when front reaches end, averaged over the length of the pipe Red: the time-averaged mixing index for the whole pipe, averaged over the length of the pipe. b) The experimental axial velocity contour for the time when the front is passing the location of UDV probe. The data are distorted because of the avoid less noises and perturbations near the walls so they are removed.

$$\mathrm{MI}_i(x,t) = \sqrt{\frac{\sum_{i=1}^{N} (C(i) - C_{\max})^2}{N}},$$

i: pixel number on diameter direction
N: total number of pixels

Effects of pipe axial rotation

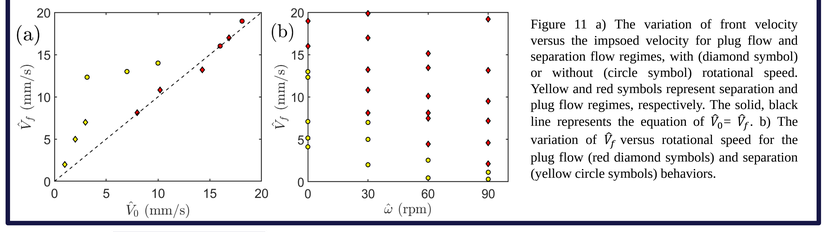

Figure 11 a) The variation of front velocity versus the imposed velocity for plug flow and separation flow regimes, with (diamond symbol) or without (circle symbol) rotational speed. Yellow and red symbols represent separation and plug flow regimes, respectively. The solid, black line represents the equation of $\hat{V}_0 = \hat{V}_f$. b) The variation of $\hat{V}_f$ versus rotational speed for the plug flow (red diamond symbols) and separation (yellow circle symbols) behaviors.

References

[1] A. Maleki and I. Frigaard, "Primary cementing of oil and gas wells in turbulent and mixed regimes," *J. Eng. Math.*, 2017.

[2] S. Lyu, M. Izadi, and S. M. Taghavi, "Exchange flows in axially rotating pipes," *Phys. Rev. Fluids*, 2020.

[3] A. Amiri, F. Larachi, and S. M. Taghavi, "Displacement flows in periodically moving pipe: understanding multiphase flows hosted in oscillating geometry," *Chem. Eng. Sci.*, 2017.

[4] S. Lyu and S. M. Taghavi, "Stratified flows in axially rotating pipes," *Phys. Rev. Fluids*, 2018.

[5] S. Lyu and S. M. Taghavi, "Viscoplastic displacements in axially rotating pipes," *J. Non-Newtonian. Fluid Mech.*, 2020.

[6] S. Akbari and S. M. Taghavi, "From breakup to coiling and buckling regimes in buoyant viscoplastic injections," *J. Fluid Mech.*, 2022.

Acknowledgments

INNOVATION.CA CANADA FOUNDATION FOR INNOVATION | FONDATION CANADIENNE POUR L'INNOVATION

NSERC CRSNG

Chaires de recherche du Canada | Canada Research Chairs

Canada